

# In Vitro Investigation into Plasmonic Photothermal Effect of Hollow Gold Nanoshell Irradiated with Incoherent Light

Armin Imanparast<sup>1,2</sup>, Neda Attaran<sup>3</sup>, Ameneh Sazgarnia<sup>1,2\*</sup>

1. Medical Physics Research Center, Faculty of Medicine, Mashhad University of Medical Sciences, Mashhad, Iran

2. Department of Medical Physics, Faculty of Medicine, Mashhad University of Medical Sciences, Mashhad, Iran

3. Assistant Professor of Organic Chemistry, Applied Biophotonics Research Center, Science and Research Branch, Islamic Azad University, Tehran, Iran

## ARTICLE INFO

### Article type:

Original Article

### Article history:

Received: Dec 17, 2017

Accepted: Jan 10, 2018

### Keywords:

Polyethyleneglycol

Nanoshell

Photothermal Therapy

Incoherent Light

## ABSTRACT

**Introduction:** Hollow gold nanoshells (HAuNS) are one of the most attractive nanostructures for biomedical applications due to their interesting physicochemical properties. This study sought to evaluate the plasmonic photothermal effect of HAuNS irradiated with incoherent light on melanoma cell line.

**Materials and Methods:** After the synthesis of nanostructures, the temperature changes of HAuNS and polyethylene glycol stabilized HAuNS (HAuNS-PEG) were evaluated at different irradiation dose levels. After determining the potential cytotoxicity of the agents, the DFW cells were irradiated by incoherent light with and without the nanostructures at different exposure doses with two spectral bands of  $670\pm 25$  nm and  $730\pm 25$  nm. Finally, the rate of the cell survival was determined by 1-Methyltetrazole-5-Thiol assay 24 h after irradiating.

**Results:** The HAuNS, HAuNS-PEG, and light exposure did not have any significant effect on the cell survival, individually. Stabilizing with PEG led to an increase in size and decreased their polydispersity index, zeta potential, and conductivity. The slopes of temperature and cell death caused by 730 nm were greater than 670 nm when the cells were irradiated in the presence of nanostructures. These changes became more significant with increasing the dose of exposure and HAuNS (or HAuNS-PEG) concentration. The lowest cell survival occurred in the concentration of 250  $\mu\text{g/ml}$  of nanostructures and an exposure dose of 9 min ( $P < 0.05$ ).

**Conclusion:** the HAuNS-PEG significantly reduced its conductivity that leads to decreased plasmonic photothermal effect. Additionally, using an incoherent light with more spectral overlap for irradiating the nanostructures increased its thermal effects.

### ► Please cite this article as:

Imanparast A, Attaran N, Sazgarnia A. In Vitro Investigation into Plasmonic Photothermal Effect of Hollow Gold Nanoshell Irradiated with Incoherent Light. Iran J Med Phys 2018; 15: 161-168. 10.22038/ijmp.2018.27289.1304.

## Introduction

Photothermal therapy is one of the less invasive methods used to fight cancer, which has attracted more attention in recent years. Its strategy is based on the production of heat following the exposure of light (from the visible to near-infrared region (NIR)). Typically, in the process of photothermal treatment, light-absorbing molecules (photosensitizers) such as porphyrins are used.

By injecting this synthetic material into the tumor tissue, the energy conversion efficiency, in case of heat from light, increased than the natural chromophore [1, 2]. Gold nanomaterials exhibit higher optical absorption efficiency in comparison to the organic dye molecules. Electrons become excited by irradiating these nanomaterials using a specific electromagnetic field [3].

The rapid return of the stimulated electrons to the ground state causes local heating, which kills malignant cells. This photothermal therapy induced

by metal nanomaterials is called plasmonic photothermal therapy (PPTT) [4]. Gold nanostructure are one of the most important mediators used in this method due to biocompatibility and the ability to adjust the plasmonic absorption peak to NIR (light absorption and scattering by the nanoparticles vary from ultra-violet to infrared regarding the shape and size of the particle), easy surface modification, small size, efficient light-to-heat conversion, and the ability to be used in combination with other therapies such as gene therapy, chemotherapy, and immunotherapy to increase antitumor activity [3, 5, 6, 7].

Spherical gold nanoparticles have an optical absorption peak of 500-600 nm. The maximum absorption wavelengths of these structures are transmitted to higher wavelengths by increasing the size of the particle [8]. Gold nanoshells are usually composed of a silica inner shell (or hollow silica core) and gold shell, which reach the absorption peak of NIR by decreasing the ratio of shell to core [9, 10]. Gold

nanorods have two absorption peaks ranging from 300-900 nm that correspond to the plasmon resonance, which can be adjusted by changing the ratio of length to width [11, 12].

Gold nanocages are porous hollow structures of gold that By increasing the diameter of the gold wall , Their absorption peak is adjustable in the range of 400 to 800 nm [13].

This study aimed to investigate the photothermal effects of hollow gold nanoshells (HAuNS) radiated with incoherent light at the boundaries of the visible region and NIR by adjusting their absorption peak.

## Materials and Methods

### Chemical

Chloroauric acid ( $\text{HAuCl}_4 \cdot 4\text{H}_2\text{O}$ ), trisodium citrate dihydrate (>99%), cobalt (II) chloride hexahydrate (99.99%), polyethylene glycol thiol (PEG-SH, MW 2000), Roswell Park Memorial Institute (RPMI) Medium 1640, trypan blue, 3-[4,5-dimethylthiazol-2-yl]-2,5-diphenyltetrazolium bromide (MTT), penicillin, trypsin-ethylenediaminepentaacetic acid, streptomycin, and sodium borohydride (99%) were purchased from Sigma-Aldrich (St. Louis, MO, USA). In all the solutions used in the synthesis of HAuNS, ultrapure deionized water was used.

### Instruments

In this study,  $\text{CO}_2$  incubator, radiometer (CONTROL-CURE IL1400, USA), Milwaukee pH/Temperature Meter (MT609, Italy), dynamic light scattering particle size analyzer (DLS) (Zetasizer Nano ZS, Malvern, UK), ultraviolet-visible (UV-vis) spectrophotometer (UNICO UV-2100, USA), enzyme-linked immunosorbent assay test (ELISA) microwell plate reader (Awareness, USA), Lumacare LC-122A (Lumacare, Newport Beach CA, USA), and incoherent light source (two probes with the wavelengths of  $670 \pm 25$  and  $730 \pm 25$  nm) were used.

### Synthesis of HAuNS-PEG

In order to produce HAuNS, oxygen-sensitive cobalt nanoparticles were first synthesized. 60 ml Ultrapure deionized water was placed in a 100 ml three-necked round bottom flask. In order to deoxygenate the water, it was heated up to the boiling point, and then the vacuum pump was used to remove the oxygen of the atmosphere of the flask. It is worth mentioning that this process was repeated three times [14].

Finally, the solution was exposed to argon flux for 45 min until the dissolved oxygen was completely discharged. Thereafter, 120  $\mu\text{l}$  of sodium citrate (0.1M) and 30  $\mu\text{l}$  of sodium tetrahydroborate (1 M) were combined in 30 ml of deoxygenated deionized water. Subsequently, by adding 30  $\mu\text{l}$  of 0.4 M solution of cobalt chloride, a brown solution was obtained.

At all the stages, argon flux was required during the synthesis process. Then, 10 ml of deionized water

containing 25  $\mu\text{l}$  of 0.1 M chloroauric acid was immediately transferred to a vortexing solution of oxygen-sensitive cobalt nanoparticles. In this reaction, the gold shell was formed on the cobalt core. Finally, the nanostructure was placed in the vicinity of air to oxidize the cobalt core and the HAuNS remained [15].

For stabilizing the HAuNS with PEG, 100  $\mu\text{l}$  of aqueous solution of PEG was added to 9.9 ml of the HAuNS solutions, and the obtained solutions were incubated at the room temperature for 1 h using a magnetic stirrer. The solutions were then centrifuged at 700g for 15 min. The supernatant was slowly discarded to remove excess PEG, and then 10 ml of Phosphate Buffered Saline (PBS) solution was added.

### Characterization of Nanostructures

The surface plasmon resonance spectra of HAuNS and HAuNS-PEG were recorded by an UV-vis spectrophotometer using a 2 mm thick quartz cuvette. The particle size, zeta potential, conductivity, and polydispersity index (PDI) were determined using a DLS.

### Thermal Behavior of the Nanostructures

To evaluate the thermal properties of HAuNS and HAuNS-PEG, 200  $\mu\text{l}$  of these nanostructures in different concentrations (75, 125, and 250  $\mu\text{g}/\text{ml}$ ) were suspended in a 96-well plate and irradiated at various exposure doses of light (4, 12, and 35  $\text{J}/\text{cm}^2$ ) with constant output power density of 65  $\text{mW}/\text{cm}^2$ . The temperature changes of the HAuNS and HAuNS-PEG samples were measured by a digital thermometer.

### Cell Culture and Cytotoxicity Assay

DFW melanoma cell line (Pasture Institute, Tehran, Iran) was cultured in RPMI 1640 containing 10% fetal bovine serum, penicillin (100 units/ml), and streptomycin (100  $\mu\text{g}/\text{ml}$ ). The cells were incubated at 37°C in the atmosphere of 5%  $\text{CO}_2$ . The DFW cells were seeded into 96-well plates containing 200  $\mu\text{L}$  of 10% medium with the density of 7500 cell/well and cultured in  $\text{CO}_2$  incubator.

After 24 h, the old medium was replaced with 200  $\mu\text{l}$  of fresh medium containing HAuNS and HAuNS-PEG with different concentrations and incubated for 4 h. The media were removed and replaced with 100  $\mu\text{l}$  of serum-free medium, and 20  $\mu\text{l}$  of MTT solution (5 mg/ml) was added in dark environment and after covering the plate with an aluminum foil. Thereafter, it was again placed in the incubator for 4 h. Then 200  $\mu\text{L}$  of dimethyl sulfoxide was added to dissolve the insoluble formazan. The absorption peak was measured with an ELISA microwell plate reader with the wavelength of 570 nm. Cell survival in treated cells, was calculated relative to the control group.

## In Vitro Experiments

The DFW cells were seeded into 24-well plates containing 500  $\mu\text{l}$  of 10% medium with the density of  $7.5 \times 10^4$  cell/well and cultured in  $\text{CO}_2$  incubator for 24 h. Then, the old medium was replaced with 500  $\mu\text{l}$  of fresh medium containing HAuNS and HAuNS-PEG with different concentrations of 75, 125, and 250  $\mu\text{g}/\text{ml}$ . After 4 h of incubation, the cells were washed three times with PBS to remove the unbound excess of HAuNS (or HAuNS-PEG), and 250  $\mu\text{l}$  of 3% fresh culture medium was added to each well.

The cells were irradiated at different exposure doses of light with the wavelengths of 670 and 730 nm. Subsequently, 250  $\mu\text{l}$  of the 17% culture medium was added to each well and incubated for 24 h. Furthermore, the cell viability was measured using the MTT assay.

## IC50 and ED50 Calculation

To compare the therapeutic efficacy of different therapeutic conditions, the exposure dose 50% (ED50) index (the amount of optical exposure required to cause cell death was 50%), and the inhibitory concentration 50% (IC50) index (the amount of concentration required to cause cell death was 50%) were determined.

## Statistical Analysis

The survival curves of the treatment groups were compared using Excel\_2016 software. To test the normality of the data, the non-parametric Kolmogorov-Smirnov test was used. After that, Tukey test following one-way analysis of variance was employed to compare the differences between the means. These tests were applied in the SPSS software version 20. In all the

measurements, P-value less than 0.05 was considered statistically significant.

## Results

### Physical Characteristics of the nanostructures

HAuNS was synthesized by galvanic displacement of oxygen-sensitive cobalt nanoparticles after rapid reaction with a golden salt solution according to the method of Schwartzberg et al. (Figure 1.A) [15]. The physical properties of HAuNS were evaluated using the DLS method. As demonstrated in Table 1, the average size, PDI, zeta potential, and conductivity of the HAuNS were determined to be 72 nm, 0.29, -24 mV, and 0.241 mS/cm, respectively.

The stabilizing of HAuNS with PEG resulted in a significant increase in colloidal stability, so that no aggregation was observed at room temperature for up to 5 months. Additionally, the physical characteristics of HAuNS-PEG such as the average size, PDI, zeta potential, and conductivity were 82 nm, -19 mV, 0.25, and 0.007 mS/cm, respectively. Despite the optical emission spectrum from light source with a wavelength of 670 and 730 nm had approximately the same distance with a HAuNS absorption peak (700 nm), they had different effects on the temperature changes of HAuNS.

The overlapping surface of the emission spectrum from a light source with a nanoparticle absorption spectrum was greater with the wavelength of 730 nm in comparison to 670 nm (Figure 1.B). Regarding the results, stabilizing the HAuNS with PEG had no effect on the absorption peak. The temperature changes of HAuNS were determined in different concentrations and at diverse doses of exposure.

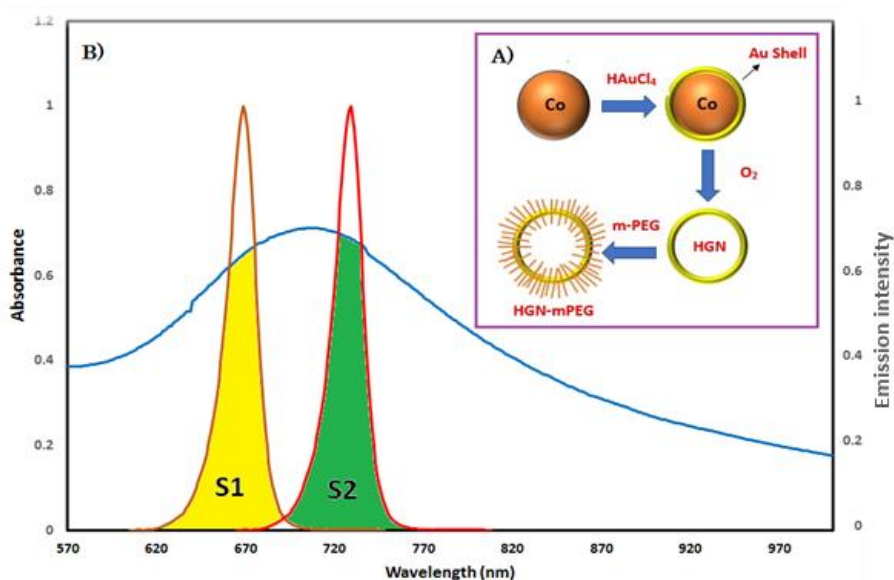


**Figure 1.** A) The steps of stabilizing the hollow gold nanoshell (HAuNS) with polyethylene glycol B) Absorbance spectrum of nanostructures and light source emission spectrum. S1 and S2 are related to the surface of the overlapping emission wavelength of 670 nm and 730 nm with the absorption spectra of HAuNS. (Emission intensity data was normalized to 1)

**Table 1.** Physical characteristics of HGN and HGN-PEG

Nanoparticle	Size (nm)	Zeta-potential (mV)	PDI	Conductivity(mS/cm)
HGN	43 ± 2.21	-24 ± 1.34	0.29 ± 0.028	0.241 ± 0.013
HGN-PEG	58 ± 1.91	-19 ± 1.9	0.25 ± 0.022	0.007 ± 0.001

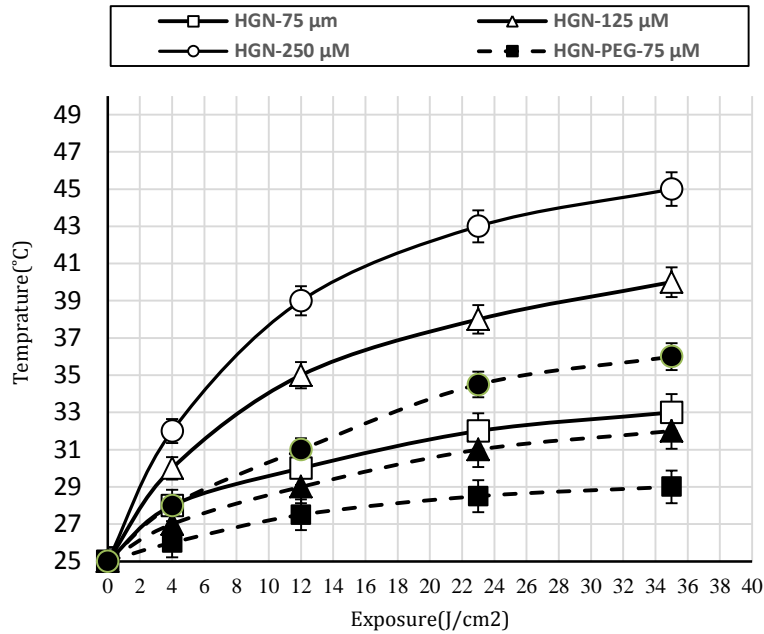


**Figure 2.** Temperature variations of different concentrations of hollow gold nanoshells (HAuNS) and HAuNS-polyethylene glycol in terms of exposure dose with the wavelength of 670 nm

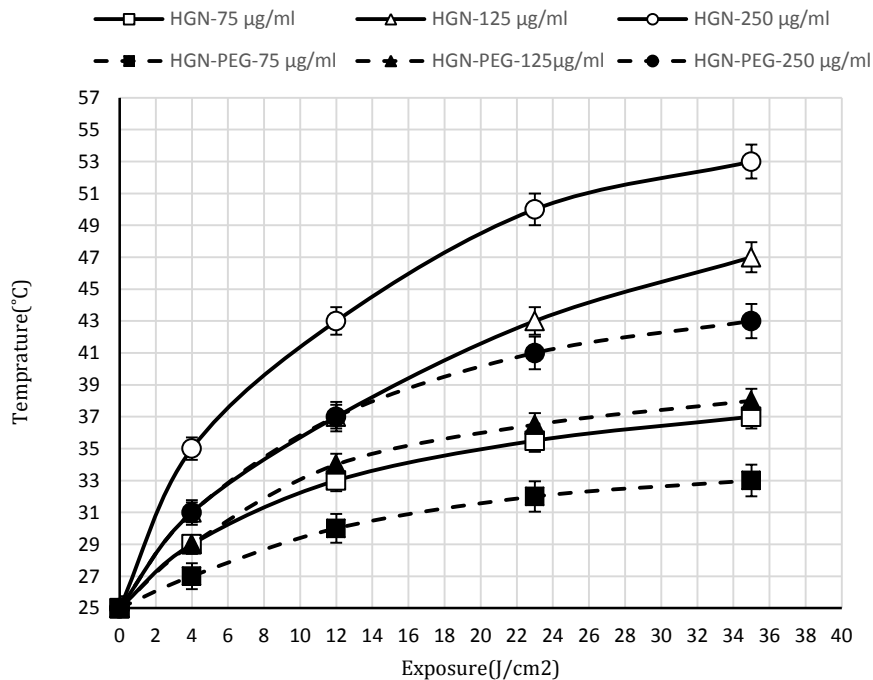


**Figure 3.** Temperature variations of different concentrations of hollow gold nanoshells (HAuNS) and HAuNS-polyethylene glycol in terms of exposure dose with the wavelength of 730 nm

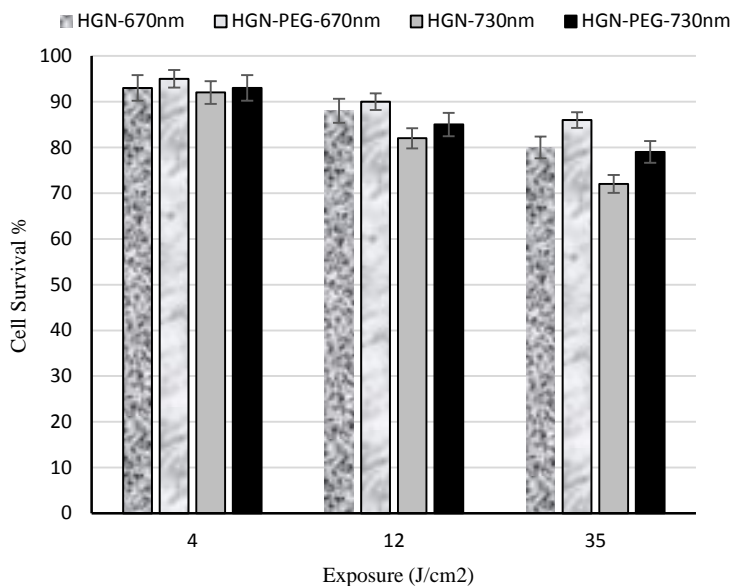


**Figure 4.** The rate of cell survival in the presence of the nanostructures at different exposure doses of light in the concentration of 75  $\mu\text{g/ml}$

By increasing the dose of exposure, the temperature of the nanostructures containing different concentrations increases with a different gradient. After 9 min of irradiation at the dose of 35  $\text{J/cm}^2$  and the concentrations of 75, 125, and 250  $\mu\text{g/ml}$ . Regarding the mentioned concentrations, the final temperatures were 33°C, 40°C, and 45°C with the wavelength of 670 nm and 37°C, 47°C, and 53°C with the wavelength of 730 nm, respectively.

However, these temperature variations were different for the HAuNS-PEG. After 9 min of exposure of light in the concentrations of 75, 125, and 250  $\mu\text{g/ml}$ , the final temperature was 29°C, 32°C, and 36°C with the wavelength of 670 nm and 33°C, 38°C, and 43°C with the wavelength of 730 nm, respectively (figures 2 and 3). Moreover, HAuNS-PEG (with the same concentration and similar exposure conditions) had a lower temperature gradient than HAuNS. These differences might be due to diverse physical properties of these structures.

As presented in Table 1, stabilizing the HAuNS with PEG led to a significant reduction in their conductivity. In other words, the PEG layer acted as an insulation and reduced the temperature incremental slope.

### The Results of Treatment Groups

In this study, four groups were assessed that were treated with HAuNS and the wavelength of 670 nm, HAuNS-PEG and the wavelength of 670 nm, HAuNS and the wavelength of 730 nm, and HAuNS-

PEG with the wavelength of 730 nm, respectively. The effect of light exposure with the mentioned wavelengths on the mentioned structures in different concentrations and at diverse irradiation doses was evaluated in all the groups.

The percentage of cell survival in the presence of HAuNS in the concentration of 75  $\mu\text{g/ml}$  and at different doses of exposure is shown in Figure 4. As the results indicated, there was no significant difference between the groups at the exposure dose of 4  $\text{J/cm}^2$ . In all treatment conditions, cell survival was higher than 90%. The rate of cell death increased along with the dose of exposure in the group treated with HAuNS with the wavelength of 730 nm, and there was a significant difference between the groups.

The lowest cell death was observed in the group who were treated with HAuNS-PEG with the wavelength of 670 nm. There was no significant difference between the other two groups who were treated with HAuNS with the wavelength of 670 nm and HAuNS-PEG with the wavelength of 730 nm. As demonstrated in Figure 5, cell survival generally decreased by increasing the dose of exposure in the concentration of 125  $\mu\text{g/ml}$ . The highest rate of cell death was related to the group treated with HAuNS with the wavelength of 730 nm; furthermore, the lowest rate of cell death was observed in the group treated with HAuNS-PEG with the wavelength of 670 nm.

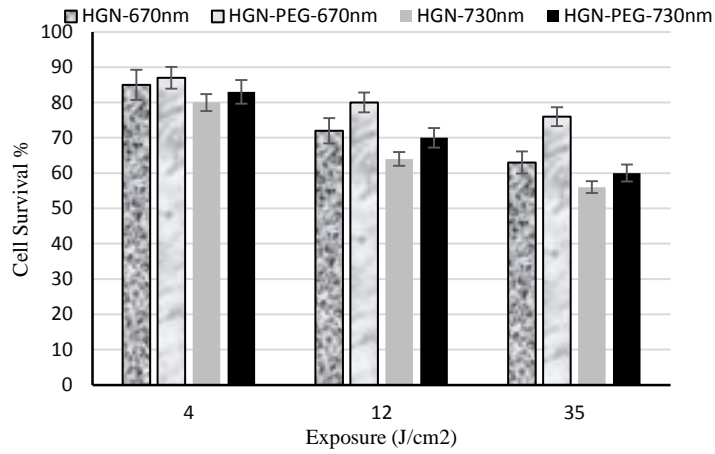


Figure 5. The rate of cell survival in the presence of nanostructure at different doses of exposure in the concentration of 125 µg/ml

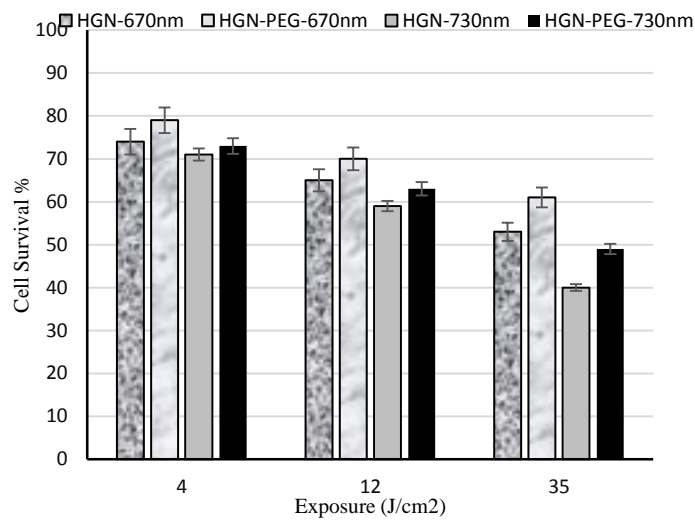


Figure 6. The rate of cell survival in the presence of nanostructure at different doses of exposure in the concentration of 250 µg/ml

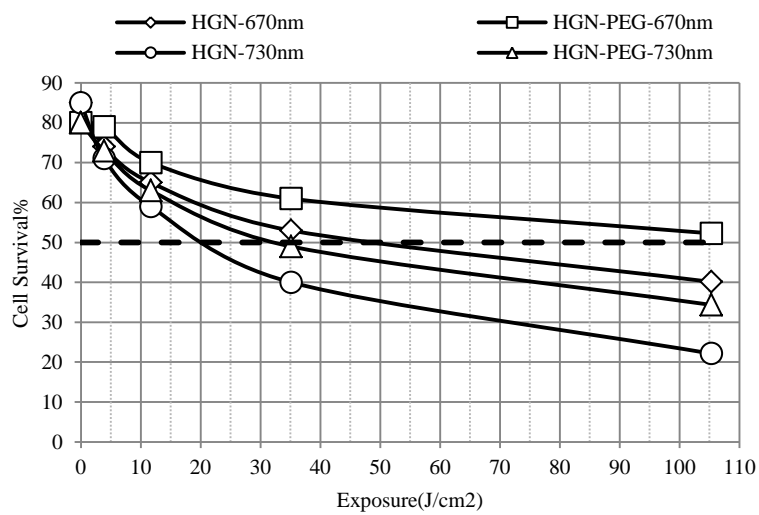


Figure 7. The rate of cell survival in terms of light exposure. In this chart, the ED50 index was compared.

**Table 2 .** IC50 and ED50 of Nanostructure

	HGN-670	HGN-PEG-670	HGN-730	HGN-PEG-730
IC50 ( $\mu\text{gr/ml}$ )	289*	348*	165	240
ED50** ( $\text{J/cm}^2$ )	48	124*	20	33

\* After obtaining the best describing curve equation, extrapolation was performed.

\*\* At a concentration of 250  $\mu\text{gr/ml}$  was calculated. At concentrations below 250  $\mu\text{gr/ml}$ , in all Exposure conditions, cell death was less than 50%.

Moreover, the rate of cell survival decreased with increasing the dose of exposure in the concentration of 250  $\mu\text{g/ml}$  (Figure 6). In addition, the rate of cell death in the group treated with HAuNS with the wavelength of 730 nm was higher than the other groups. Regarding the results, there was a direct relationship between the rate of cell death and the concentration of nanoparticles and the irradiation dose.

Additionally, the slope of temperature changes was dependent on the dose of exposure and concentration. Nevertheless, increasing the exposure dose with each wavelength did not result in the same increase in the temperature. According to Table 2, the lowest levels of IC50 and ED50 were related to the group treated with HAuNS with the wavelength of 730 nm, which might be due to the greater phototoxicity of HAuNS with the wavelength of 730 nm compared to the other nanostructures. Moreover, stabilizing the nanostructure with PEG resulted in an increase of IC50 and ED50 and reduced the phototoxicity (figures 7 and 8).

## Discussion

Schwartzberg et al. presented a report on the production of HAuNS for the first time. They demonstrated that the peak of surface plasmonic absorption of HAuNS can be adjusted by changing the inner diameter and thickness of the gold shell in the range of 550 to 820 nm [15]. Abbasi et al. examined the optical absorption efficiency of gold nanoshell with different cores. Simulations showed that HAuNS as the best option in PPTT. Most important reasons for this choice included the optical tunability, absorption efficiency, low dose of nanomaterials, the compatible core (hollow) with body tissues, and cost-efficiency [16]. Jian Yu et al. synthesized the HAuNS-PEG as the carrier of doxorubicin. They used this nanostructure as an interface for PPTT using infrared lasers. In fact, a dual-purpose therapeutic approach was proposed as photothermal and chemotherapy [17]. Nonetheless, in this study, the effect of overlaying the optical fiber bandwidth with nanostructured absorption spectra and surface nanostructured conductivity on the temperature rise and photothermal effects were evaluated for the first time.

The most important condition for producing a photothermal effect is the use of a long-wavelength light source; therefore, the light source bandwidth

can stimulate the surface plasmon resonance of the nanostructure. However, another important factor that was discussed in this study was the level of overlapping bandwidth of a light source with an absorption spectrum of nanoparticles.

The above factors were related to the ability of a nanostructure to absorb energy. However, another factor that leads to the optimal use of the potential of a nanostructure in the occurrence of a photothermal effect was related to the ability of a stimulated nanostructure to share the heat with its surrounding.

In other words, if the nanostructured heat exchange was weak, its ability to create photothermal effects would decrease. Even if photothermal effects are predicted.

The absorption spectra of the HAuNS and HAuNS-PEG are similar in terms of spectrophotometric analysis. Nevertheless, the effect of photothermal process, the HAuNS-PEG acts poorly in the exchange of heat than HAuNS due to the fact that PEG layer has several hundred times less conductivity. Therefore, it exhibits less temperature variation by applying light exposure and fewer photothermal effects.

It is anticipated that using pH-sensitive types of PEG as a stabilizing agent for nanoparticles rather than common PEG can prevent the unpleasant consequences of reducing photothermal effect.

## Conclusion

One of the most important nanostructures in the field of cancer treatment and diagnosis is HAuNS. In this study, the effective factors in the occurrence of thermal changes in HAuNS were evaluated. By changing the ratio of gold shell thickness to hollow core diameter, the plasmonic absorption peak of the nanoshell shifted towards longer wavelengths in the visible and infrared regions. According to the literature, near infrared laser therapy (or a long-wavelength light source) that overlaps with the plasmonic absorption peak of the photothermal agent (or nanoparticle) was identified as the key treatment factor.

In this study, two other important factors were proposed to improve the process of photothermal therapy. The first factor was the need for a high thermal conductivity of nanostructure. This factor was ignored due to applying surface modifications to convert the nanostructure to a biocompatible agent. For example, stabilizing the nanostructure with PEG resulted in a remarkable reduction of its thermal

conductivity, which reduced the photothermal effect. The second factor was providing maximum overlap area between the emission spectrum of the light source and the absorption spectra of nanostructures.

In order to expand research in the same field as this study, it is suggested that, the use of physical simulation software, the effects of the shell thickness to core ratio, the impact of nanostructure size on the photothermal process, and the effect of different physical fields in vitro and in vivo were evaluated. Moreover, these nanostructures can be used as a carrier of different photosensitizers due to their optical properties.

### Acknowledgment

This paper is a part of Master thesis in the field of medical physics. The authors would like to thank the Research Deputy of Mashhad University of Medical Sciences, Mashhad, Iran, for their financial support.

### References

- Ban Q, Bai T, Duan X, Kong J. Noninvasive photothermal cancer therapy nanoplatfoms via integrating nanomaterials and functional polymers. *Biomaterials Science*. 2017;5:190-210.
- Zou L, Wang H, He B, Zeng L, Tan T, Cao H, et al. Current Approaches of Photothermal Therapy in Treating Cancer Metastasis with Nanotherapeutics. *Theranostics*. 2016;6:762-72.
- Hwang S, Nam J, Jung S, Song J, Doh H, Kim S. Gold nanoparticle-mediated photothermal therapy: current status and future perspective. *Nanomedicine*. 2014;9:2003-22.
- Huang X, El-Sayed MA. Plasmonic photo-thermal therapy (PPTT). *Alexandria Journal of Medicine*. 2011;47:1-9.
- Choi J, Yang J, Jang E, Suh JS, Huh YM, Lee K, et al. Gold nanostructures as photothermal therapy agent for cancer. *Anti-cancer agents in medicinal chemistry*. 2011;11:953-64.
- Kafshdooz L, Kafshdooz T, Razban Z, Akbarzadeh A. The application of gold nanoparticles as a promising therapeutic approach in breast and ovarian cancer. *Artificial cells, nanomedicine, and biotechnology*. 2016;44:1222-7.
- Nicol JR, Dixon D, Coulter JA. Gold nanoparticle surface functionalization: a necessary requirement in the development of novel nanotherapeutics. *Nanomedicine (London, England)*. 2015;10:1315-26.
- Huang X, El-Sayed MA. Gold nanoparticles: Optical properties and implementations in cancer diagnosis and photothermal therapy. *Journal of Advanced Research*. 2010;1:13-28.
- Lal S, Clare SE, Halas NJ. Nanoshell-enabled photothermal cancer therapy: impending clinical impact. *Accounts of chemical research*. 2008;41:1842-51.
- Singhana B, Slattery P, Chen A, Wallace M, Melancon MP. Light-activatable gold nanoshells for drug delivery applications. *AAPS PharmSciTech*. 2014;15:741-52.
- Chen J, Liang H, Lin L, Guo Z, Sun P, Chen M, et al. Gold-Nanorods-Based Gene Carriers with the Capability of Photoacoustic Imaging and Photothermal Therapy. *ACS applied materials & interfaces*. 2016;8:31558-66.
- Jiang T, Zhang B, Shen S, Tuo Y, Luo Z, Hu Y, et al. Tumor Microenvironment Modulation by Cyclopamine Improved Photothermal Therapy of Biomimetic Gold Nanorods for Pancreatic Ductal Adenocarcinomas. *ACS applied materials & interfaces*. 2017;9:31497-508.
- Xia Y, Li W, Cobley CM, Chen J, Xia X, Zhang Q, et al. Gold nanocages: from synthesis to theranostic applications. *Accounts of chemical research*. 2011;44:914-24.
- Patrick WA, Wagner HB. Method for Complete Deoxygenation of Water. *Analytical Chemistry*. 1949;21:752-3.
- Schwartzberg AM, Olson TY, Talley CE, Zhang JZ. Synthesis, Characterization, and Tunable Optical Properties of Hollow Gold Nanospheres. *The Journal of Physical Chemistry B*. 2006;110:19935-44.
- Abbasi S, Servatkah M, Keshtkar MM. Advantages of using gold hollow nanoshells in cancer photothermal therapy. *Chinese Physics B*. 2016 Jun 25;25(8):087301.
- You J, Zhang G, Li C. Exceptionally high payload of doxorubicin in hollow gold nanospheres for near-infrared light-triggered drug release. *ACS nano*. 2010 Feb 1;4(2):1033-41.